Bi-Component Silicone 3D Printing with Dynamic Mix Ratio Modification for Soft Robotic Actuators

Brice Parilusyan[1,2,3], Alina-Elena Nicolae[1], Thomas Batigne[3]
Clément Duhart[1], and Marcos Serrano[2]

***Abstract*— Pneumatically operated soft actuators are increasingly researched due to their fabrication simplicity, actuation capabilities, and low production cost. Depending on the Soft Pneumatic Actuator (SPA) objective, its design can be modified to reach new bending angles or increase its actuation strength. However, increasing the abilities of Soft Pneumatic Actuators (SPAs) requires increasing the complexity of their air cavities or using multiple materials with different mechanical stiffness. Both solutions complexify the fabrication of SPAs, reducing their primary benefits of manufacturing simplicity and low production cost. This paper presents a novel additive manufacturing fabrication process incorporating multiple mechanical stiffnesses using a single bi-component soft material. This process aims to integrate multiple bending angles with multi-channel SPAs without increasing their manufacturing complexity. Our process uses a dynamic modification of the bi-component silicone mix ratio to generate the desired mechanical properties of the material. Modifying the mix ratio allows us to control the material's cure time and mechanical properties, such as its final stiffness. We found that using a single 30 shore-A bi-component silicone, we could achieve several stiffness values with different reticulation times and levels of stickiness. Using these shore ranges and our fabrication process, we built several SPAs. We explored how the printing orientation of the SPAs modifies its bending actuation using our fabrication process to illustrate the capabilities of our approach.**

Fig. 1: SPAs printed with silicone dynamic mix ratio modification layer-by-layer. Left) Printed standing resulting in linear extension when inflated (currently inflated). Right) Printed flat resulting in angular deformation when inflated (currently inflated). Center) Multi-channel actuators printed flat, resulting in increased bending control (not inflated).

I. INTRODUCTION

Pneumatic actuators are among the most common actuators in soft robotics [1]. Soft Pneumatic Actuators (SPAs) work by using air cavities to create movements when inflated. Cavities' position on the actuator, shape, and size make it possible to define the orientation and strength of the deformation of the soft actuator during inflation [2]. Compressed air allows for a decent reaction speed and the use of many different materials [3]. However, increasing the Degree Of Freedom (DOF) of the SPAs leads to the multiplication of cavities on the actuator, with dedicated air channels [4]–[6]. This increases the overall structure complexity, requiring new tools to model the soft actuator according to the desired constraints [7], [8]. These multi-channels SPAs become harder to manufacture and lead to a consequent increase in volume due to a large number of cavities [9].

Alternative methods have been explored to reduce the size and number of cavities to optimize SPAs. A first researched solution involves locally modifying the material's mechanical properties that compose the soft actuator [10]. Using several materials allows accurate modifications of the soft actuator's local properties, thus creating stronger deformation zones [11], [12]. The creation of multi-material SPAs has encouraged the use of 3D printing for their manufacture [13], [14] as it can integrate several materials [15], [16] with fewer steps than molding. However, the multi-material printing of a single actuator requires merging several printing processes with non-compatible settings (temperature, solidification time). These limitations increase the fabrication complexity and reduce the number of shapes available. A second method is to use 3D printing to modify specific structural parameters of the SPAs [17], such as the wall's thickness [18] or layer height [19]. These structural modifications impact the SPAs deformation locally during inflation. Still, they require modifying the 3D model of the soft actuator, which is time-consuming without adapted tools [20] and can lead to 3D shapes challenging to print. To the best of our current knowledge, no solution exists to integrate local modifications of the SPA's mechanical properties to control its behavior during inflation with a single material and without increasing the complexity of the fabrication or modeling process.

This paper presents an approach to integrate local stiffness variations in SPAs during the printing process using a single bi-component silicone without modification of the 3D model. Bi-component silicone results from mixing two

*This work was supported by the french company Lynxter [23]
[1]Léonard de Vinci Pôle Universitaire, Research Center, France
[2]University of Toulouse 3, IRIT - Elipse, France
[3]Lynxter, 3D-printer manufacturer, France

silicone components with a specific mix ratio to obtain the desired shore. Modifying this mix ratio can lead to shore reduction, increased stickiness, and stiffness reduction. More precisely, our approach dynamically changes the mix ratio of bi-component silicone during printing to create local shore variation. By studying the mechanical properties of the silicone with several mix ratios, we select the ratios that reduce shore without causing a high reduction of the silicone quality. Then, we dynamically changed the mix ratio during printing to integrate local modification of the mechanical properties of the silicone, which will define the SPAs behavior during inflation. Before printing, this approach requires running a script to define the layers with a modification of the silicone's mix ratio, thus, moving the definition of SPAs actuation from the 3D modeling phase to the fabrication phase. Our approach allows the creation of SPAs with lower complexity design and higher deformation capabilities.

The main contributions of this paper are as follows:

- A novel SPA fabrication approach based on the dynamic modification of bi-component silicone's mix ratio to integrate local shore variation during silicone printing and its implementation.
- An experimental characterization of the material stiffness according to the bi-component silicone mix ratio.
- A study of the impact of the printing orientation on the SPAs behavior using our fabrication approach.

We first introduce the working principle of the fabrication approach in section II. Section III evaluates the tensile strength variation as a function of the bi-component silicone mix ratio to determine the best ratio to use. Next we explore and characterize SPAs built with our fabrication approach in section IV. Finally, section V concludes and presents future works on applying bi-component silicone mix-ratio variation.

II. Variable Shore Printing

This section introduces our fabrication approach to create Soft Pneumatic Actuators (SPAs) with multiple mechanical properties using a single bi-component silicone without modification of the 3D model. We present the general principle of our approach, the manufacturing process, and the slicing method.

A. General Principle

SPAs bending behaviors are often linked to their shape (cavities, wall thickness) when inflated. The only method to customize this bending behavior without modification of the 3D model is to incorporate several mechanical properties in different areas of the model. This is usually carried out by inserting multiple materials in the same part. This multi-material printing increases fabrication complexity, a lower success rate, and a higher cost [21]–[23].

Our fabrication process uses the properties of bi-component silicone to dynamically integrate several mechanical properties with a single material. Bi-component silicone is one of the primary materials used for SPAs fabrication. This is a fluid material whose mechanical properties come from chemical reticulation. The reticulation process depends on mixing the two silicone components named A and B with a specific ratio. A variation of the ratio changes the properties of the silicone and can be used to integrate several mechanical properties with the same material. For 3D printing, we use a static mixer to mix the bi-component silicone during printing. Our approach consists of dynamically changing the mixing ratio of the bi-components during printing to generate changes in the silicone properties on several parts of the printed piece, as presented in Figure 2. Modifying the silicone properties allows this system to integrate bending actuation when inflated to SPAs.

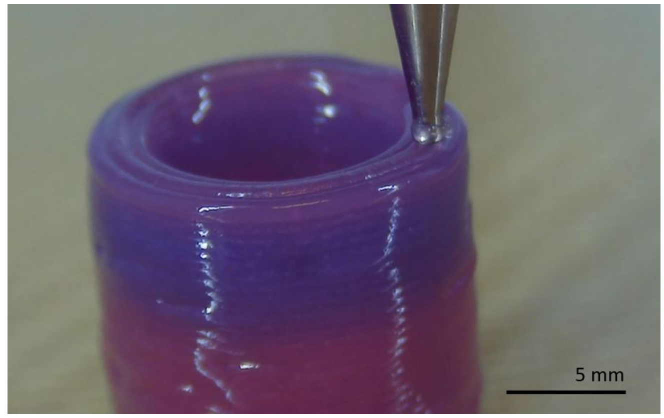

Fig. 2: Silicone printing with mix ratio variation. The A and B components of the silicone have different colors, allowing for the mix ratio change to be visually detected through a color shift. The mix ratio is altered dynamically during the printing process.

The first step is to characterize the material's tensile strength properties depending on the silicone ratio. Then, we select several ratios as a function of the achieved properties and their printability. Finally, we integrate the ratio modification in the G-code of the printing file using a custom script, resulting in a dynamic ratio change during printing. The mixing variation is done between layers, meaning the silicone's mechanical properties depend on the Z-axis. Thus, the orientation of the SPAs during printing will impact its bending deformation during inflation, as illustrated in Figure 3.

B. Manufacturing Process

We printed the actuators on a Lynxter S600D 3D printer [24], a modular Extrusion Additive Manufacturing (EAM) printer with a controlled printing environment. The printing material used is the DragonSkin 30 silicone from smooth-on [25], a 30-shore A bi-component silicone skin-safe, with a pot life of 45 minutes at 20°C. Fumed silica is added to each part to increase its printability for 5% of the total weight. To differentiate the components and visualize the mixing ratio, a red coloration is added for component A and a blue coloration for component B. The two silicone components are mixed during printing using a custom static mixer. A variation from red to blue through shades of purple

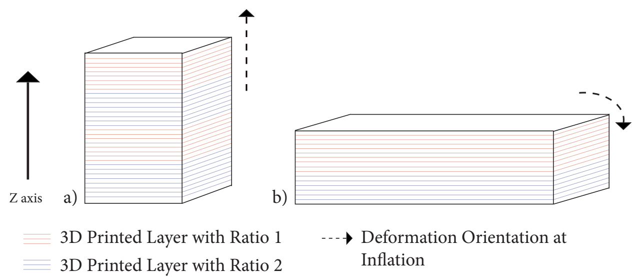

Fig. 3: Printing orientation and layer management impact on the deformation of the actuator at inflation. Ratio 1 is softer than ratio 2. a) The actuator is printed standing with a successive modification of the mix ratio, resulting in a linear extension at inflation. b) The actuator is printed flat with a ratio modification in the middle of the printing, resulting in an angular deformation at inflation.

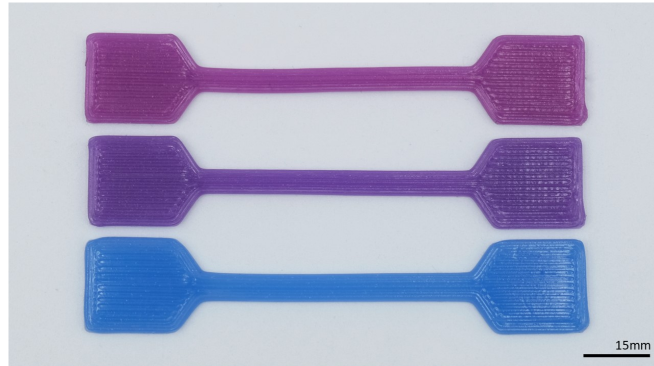

Fig. 4: Dog-bone-shaped traction test samples. Each color represents a mix ratio (red = 80%A, purple = 55%A, Blue = 15%A). The traction samples stretched part has the following dimensions: length l_0 = 60 mm, width w_0 = 5 mm, and thickness t_0 = 3 mm.

is observed depending on the mixing ratio. This variation of color indicates the area with modified properties.

The 3D model is sliced using the Simplify software [26], then the mix definition commands are added to the g-code file using a custom python script. The mix ratio change has inertia due to the purge of the static mixer. Hence we calculate the necessary length to purge the static mixer with the formula 1.

$$Dp = (B * H)/b \tag{1}$$

Where Dp is the length required to purge the static mixer volume, B is the base surface, H is the static mixer height, and b is the nozzle tip's surface.

A solution to remove this inertia is to perform a forced purge of the static mixer out of the printed part. This process is mandatory for small pieces with low amounts of materials but leads to a large amount of wasted material. For this study, we decided to let the mix ratio evolve progressively without forced purging as it had a low impact due to the size of the printed SPAs. However, the ratio change inertia will add a delay between the moment the ratio has to change and the moment the silicone extruded correspond to the expected ratio. This delay complexifies the slicing process if we expect to change the silicone properties in a specific layer area. For this reason, we decided to perform the ratio modifications during the layer-changing step only.

We first explored combining only two mix ratios with opposed mechanical properties to validate our approach. Using these two ratios simplifies the slicing parts of the SPAs as a function of the desired mechanical properties. These ratios have to be selected depending on the material used. Thus, the values for these two ratios result from the tensile strength test presented in section III.

III. Material Characterization

This section evaluates the Dragon Skin 30 bi-component silicone's mechanical resistance to traction according to the mix ratio of the silicone chemical components.

A. Evaluation Protocol

The mix ratio is defined as a % of component A, with the remaining % as component B. We studied a part A ratio variation between 10% to 90% with incremental steps of 5%. Inspired by previous research [27], four dog-bone shape samples were printed for each ratio step with the following dimensions: length l_0 = 60 mm, width w_0 = 5 mm, and thickness t_0 = 3 mm, see Fig. 4.The 50% ratio required a very short drying time of about 10 - 15 min at 25°C. As the ratios moved further away from 50%, the drying time increased until incubation at 80°C was required for 1 hour at 90% part A. To ensure the samples were reticulated at their maximum level, they were left to cure at 80° for 2 hours before the uniaxial tensile testing independently of their mix ratio. The printing time required for one sample is 15 minutes.

The uniaxial tensile strength tests were conducted with a custom uniaxial tensile machine with a load cell HX711 AD of 20kg. Each sample was pulled over a 90 mm distance limit (250% initial size) while recording the elongation and applied strength. From the data, we determined the stiffness of the samples by calculating Young's modulus value E of the material at 250% of its initial size depending on its mix ratio using the formula 2.

$$E = \frac{\sigma}{\epsilon} \tag{2}$$

The value σ is the stress calculated with the formula $\frac{F}{S}$ with F as the applied load and S as the sectional area. The value ϵ is the axial strain calculated with the formula $\frac{\Delta l}{l_0}$ with Δl as the elongation length and l_0 as the initial length.

B. Results & discussions

Fig 5 plots the result of the tensile test, which draws loading applied to the sample as a function of the amount of component A for a stretched sample at 250% of its initial size. We first observed that the stiffness of the samples decreases when we reduce the amount of component A below

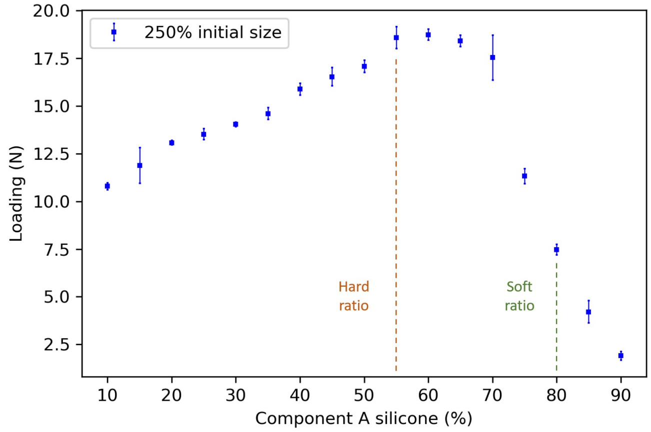

Fig. 5: Loading required to stretch the samples at 250% of their initial size as a function of their amount of component A. Each point represents the average result of the samples with standard deviation. Ratios 55% and 80% have been selected respectively as the hard and soft mix ratios. We used four samples for each point, totaling 68 samples.

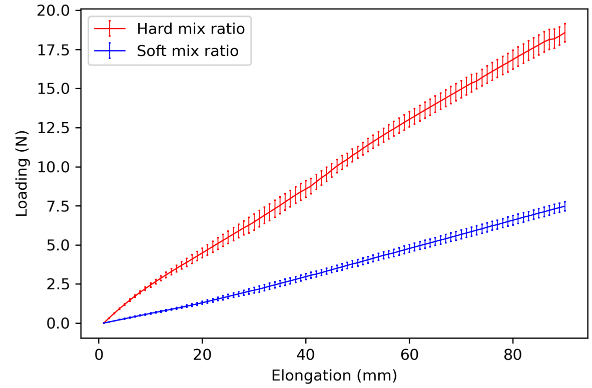

Fig. 6: Tensile test results for the component A ratio of 55% and 80%, respectively, hard and soft mix ratio. The required loading for elongation of 90 mm (250% of the initial size) is multiplied by two between the soft and hard ratio.

50%, which is the expected ratio for this silicone's normal use. However, an increase of part A between 50% to 70% of the total ratio leads to a stiffer material. Past a ratio of 70%, the stiffness value falls until the 90% ratio, where the required loading is equal to 1/9 of the loading required for the 50% ratio. We observed that a ratio of component A higher than 80% severely increases the reticulation time of the materials. Furthermore, the samples don't reticulate correctly and tend to be sticky.

We defined two mix ratios from these results: a hard and a soft ratio. The hard mix ratio corresponds to 55% of component A with a Young's modulus of 0.83 MPa with a standard deviation of 0.03 MPa. Silicone has a high stiffness value and short reticulation time with this ratio. The soft mix ratio was defined at 80% of part A with a Young's modulus of 0.33 MPa with a standard deviation of 0.01 MPa. This is the lowest value reachable with a low impact on the material's printability. With this ratio, silicone has a low stiffness value for a short reticulation time. Fig 6 summarizes the selected ratio's tensile test.

IV. Applications and Discussion

This section explores our approach's applications according to the actuator's printing orientation, which results in different deformations: angular deformation, linear extension, or multiple deformations. We discuss these applications and other aspects of our approach.

A. Angular deformation

We demonstrate an angular deformation with a rectangular actuator with dimensions of 80mm by 10mm and 10mm tall, with a central cavity of 6mm in diameter for 77 mm long. Due to its shape, printing this actuator with normal parameters should result in low inflation but no bending or extension deformation. The actuator is printed horizontally on the building plate with a ratio modification from hard to low at one-third of the print time. The resulting actuator has a third of its layer with a high stiffness value and the rest with a low stiffness value with a clear delimitation along its side, see fig 1. The actuator presents a maximum angular deformation of 25.7° at 0.8 bar before breaking, see fig 7. The combination produces an angular deformation as the soft ratio is softer than the hard ratio. However, the soft ratio has a lower mechanical resistance, leading to a low pressure bearable by the actuator before reaching its breaking point. Most actuators undergo a soft ratio's layers delamination, highlighting a reduced layer join.

B. Linear extension

We demonstrate a linear extension with a cylindrical actuator of 15 mm in diameter for 70 mm long with a central cavity of 10mm in diameter for 77 mm long. Due to its shape, printing this actuator with normal parameters should result in low inflation but no bending or extension deformation. The actuator is printed standing on the build plate with four ratio modifications from hard to soft ratio and four from soft to hard ratio. The resulting actuator has a succession of soft areas interrupted by hard areas along its length, see fig 1. The actuator presents a linear extension with a maximum value of 12 mm at 0.7 Bar before breaking, see fig 8. It represents a 17% length extension of its initial size. Increasing the length of the actuator will increase its extension value but also reduce its printability. A longer actuator requires a thicker diameter to bear the printing process.

C. Multi-channels soft actuator

Using our fabrication approach, we explored how to make a Soft Pneumatic Actuator (SPA) with multiple channels. We designed a rectangular actuator of 80mm for 10mm thick and 20mm height. The actuator has two cavities of 6mm in diameter for 77 mm long spaced of 4mm. We printed this actuator flat with a cavity on top of another.

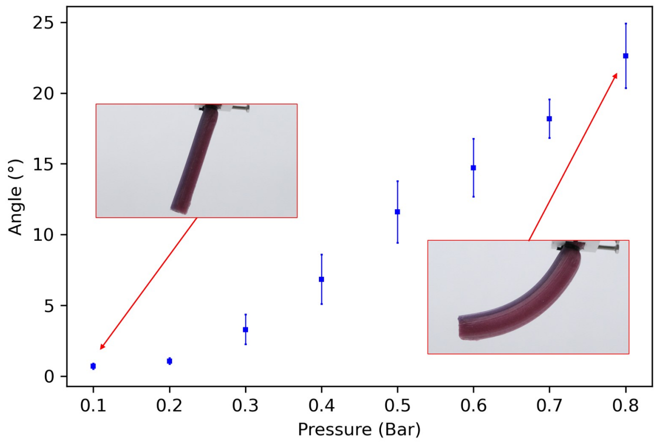

Fig. 7: The measure of the bending angle as a function of the applied internal air pressure. The red layers are the soft ratio, while the purples are the hard ratio. The measure of the actuator's angle was stopped before it reached its breaking point. We measured a maximum angular deformation of 25.7° at 0.8 bar. We tested five samples to make this graph.

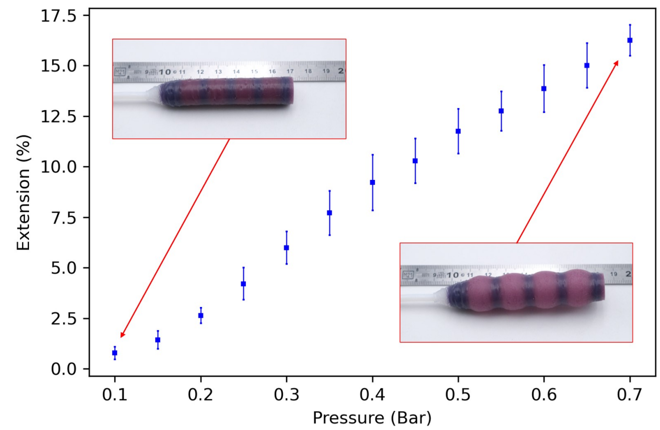

Fig. 8: The measure of the linear extension as a function of the applied internal air pressure. The red layers are the soft ratio, while the purples are the hard ratio. The measure of the actuator's extension was stopped before it reached its breaking point. We measured a maximum initial size extension of 17% at 0.8 bar with five samples tested.

Most of the layers of the actuator are printed with the soft ratio except for the ten layers between the two cavities, which are printed with the hard mix ratio, see fig 1. The resulting actuator presents an angular bending ability with the orientation depending on the inflated cavity and can reach a maximum bending angle of 16.9°, see Fig 9.

D. Discussion

Bi-component silicone is the most used material for 3D printed Soft Pneumatic Actuators (SPAs). The fabrication approach we present allows for a new way to integrate bending behaviors to SPAs using this material. This approach defines and integrates the actuation during the fabrication steps of the actuator. Thus, reducing the required work to design the actuator and accelerating the prototyping of SPAs. Our tests revealed some limitations due to our particular silicone mix, which could be easily solved by changing the type of silicone components. First, a ratio modification leads to a reduction in the silicone quality. The angular actuator we printed showed low resistance to delamination due to a weak layer joint. Second, soft ratio silicone tends to be harder to print as it requires a longer reticulation time and sticks to the nozzle more than the normal ratio of 50/50. To solve these issues, we plan to use a bi-component silicone formulated for printing, it should present better resilience to properties degradation and increased printability.

The maximum number of shapes we can make using our approach is currently limited by the printing orientation (i.e. ratio modification along the z-axis). Integrating both linear extension and angular deformation to the SPAs, would require printing the actuator with overhang, but silicone printing struggles with an overhang lower than 50° [28]. To solve this challenge, we plan to use support materials such as hydrogels to allow lower overhangs. We adopted layer-by-layer printing due to the inertia of the static mixer,

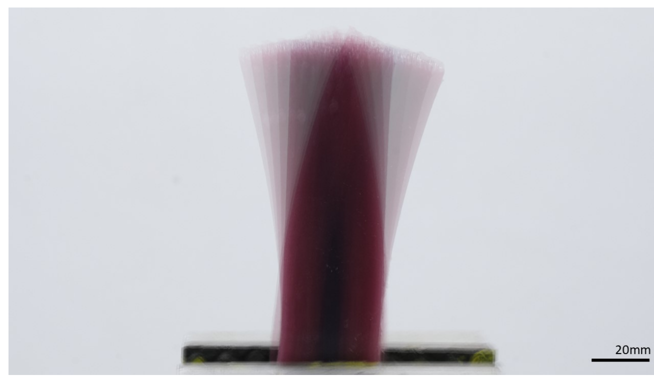

Fig. 9: Multi-channels actuator with its bending angles. The picture is a superposition of the SPA's photos with its channels at several pressure levels. The maximum bending ability reached was 16.9° at 0.8 bar.

which doesn't allow printing a precise area with a given ratio: consecutive ratio modifications tend to clog the static mixer, resulting in a ratio different from expected. We plan to use two static mixers to print the hard and soft ratios separately. This would allow printing a precise area with a particular ratio and would reduce the risk of clogging the static mixer.

V. Conclusion and Future Work

A. Conclusion

Soft Pneumatic Actuators (SPAs) present several advantages compared to other soft actuators, especially thanks to their fabrication simplicity and reaction time. Increasing the Degree Of Freedom (DOF) of SPAs is linked to increased manufacturing complexity due to managing air cavities or using multiple materials. This paper explores a printing approach for bi-component silicone's SPAs to control the deformation orientation during manufacturing rather than during its design. This process uses a dynamic change of the bi-component silicone's mix ratio to generate mechanical properties variation in the printed part. We studied how we could use this process to simplify the design of SPAs while increasing their channel quantity with the constraint of having variations only along the Z-axis. This results in SPAs being able to reach different mechanical behavior depending on their printing orientation.

B. Future work

The applications shown in this paper mainly focus on using the printing approach to generate deformations at inflation without additional air cavities. Future work will explore combining air cavities with our fabrication approach to reach higher deformation capabilities while miniaturizing the design of the SPAs.

Furthermore, we explored the impact of the printing orientation due to the static mixer inertia to change the mixing ratio of the bi-component silicone. This inertia doesn't allow the modification of the precise area of the printed part without a constant purge of the static mixer and some material waste. We plan to design a dual-printing solution to use several mixing ratios simultaneously in the same printing. The resulting solution would allow exploring how to use our fabrication process to do local stiffness modification in SPAs, thus increasing the maximum potential of the approach.

Finally, we explored using a single bi-component silicone. 3D printing of soft materials mainly focuses on silicone because this material achieves great elasticity and is durable. Several other silicones exist with different properties which could keep good mechanical properties while reducing their stiffness. We plan to experiment with other silicone formulations to find one that suits our approach best.

VI. Acknowledgment

This work was supported by an industrial research partnership with Lynxter [24]. The authors would like to thank the company for the help provided.

References

[1] E. Sachyani Keneth, A. Kamyshny, M. Totaro, L. Beccai, and S. Magdassi, "3d printing materials for soft robotics," Advanced Materials, vol. 33, no. 19, p. 2003387, 2021.

[2] B. A. W. Keong and R. Y. C. Hua, "A novel fold-based design approach toward printable soft robotics using flexible 3d printing materials," Advanced Materials Technologies, vol. 3, no. 2, p. 1700172, 2018.

[3] J. Z. Gul, M. Sajid, M. M. Rehman, G. U. Siddiqui, I. Shah, K.-H. Kim, J.-W. Lee, and K. H. Choi, "3d printing for soft robotics–a review," Science and technology of advanced materials, vol. 19, no. 1, pp. 243–262, 2018.

[4] B. Zhang, C. Hu, P. Yang, Z. Liao, and H. Liao, "Design and modularization of multi-dof soft robotic actuators," IEEE Robotics and Automation Letters, vol. 4, no. 3, pp. 2645–2652, 2019.

[5] Z. Zhakypov and A. M. Okamura, "Fingerprint: A 3-d printed soft monolithic 4-degree-of-freedom fingertip haptic device with embedded actuation," in 2022 IEEE 5th International Conference on Soft Robotics (RoboSoft). IEEE, 2022, pp. 938–944.

[6] P. Yuan and H. Tsukagoshi, "Double helical soft pneumatic actuator capable of generating complex 3d torsional motions," IEEE Robotics and Automation Letters, vol. 6, no. 4, pp. 8142–8149, 2021.

[7] A. Altelbani, H. Zhou, S. Mehrdad, F. Alambeigi, and S. F. Atashzar, "Design, fabrication, and validation of a new family of 3d-printable structurally-programmable actuators for soft robotics," IEEE Robotics and Automation Letters, vol. 6, no. 4, pp. 7941–7948, 2021.

[8] M. S. Xavier, A. J. Fleming, and Y. K. Yong, "Design and control of pneumatic systems for soft robotics: A simulation approach," IEEE Robotics and Automation Letters, vol. 6, no. 3, pp. 5800–5807, 2021.

[9] C. Premarathna, A. Kulasekera, D. Chathuranga, and T. Lalitharatne, "A novel fabrication method for rapid prototyping of soft structures with embedded pneumatic channels," in 2019 Moratuwa Engineering Research Conference (MERCon). IEEE, 2019, pp. 430–435.

[10] D. D. Arachchige and I. S. Godage, "Hybrid soft robots incorporating soft and stiff elements," in 2022 IEEE 5th International Conference on Soft Robotics (RoboSoft). IEEE, 2022, pp. 267–272.

[11] C. Aygül, J. Kwiczak-Yiğitbaşi, B. Baytekin, and O. Özcan, "Joint design and fabrication for multi-material soft/hybrid robots," in 2019 2nd IEEE International Conference on Soft Robotics (RoboSoft). IEEE, 2019, pp. 477–482.

[12] L. Smith, T. Hainsworth, Z. Jordan, X. Bell, and R. MacCurdy, "A seamless workflow for design and fabrication of multimaterial pneumatic soft actuators," in 2021 IEEE 17th International Conference on Automation Science and Engineering (CASE). IEEE, 2021, pp. 718–723.

[13] Y. L. Yap, S. L. Sing, and W. Y. Yeong, "A review of 3d printing processes and materials for soft robotics," Rapid Prototyping Journal, vol. 26, no. 8, pp. 1345–1361, 2020.

[14] R. L. Truby, M. Wehner, A. K. Grosskopf, D. M. Vogt, S. G. Uzel, R. J. Wood, and J. A. Lewis, "Soft somatosensitive actuators via embedded 3d printing," Advanced Materials, vol. 30, no. 15, p. 1706383, 2018.

[15] T. Calais, N. D. Sanandiya, S. Jain, E. V. Kanhere, S. Kumar, R. C.-H. Yeow, and P. Valdivia y Alvarado, "Freeform liquid 3d printing of soft functional components for soft robotics," ACS Applied Materials & Interfaces, vol. 14, no. 1, pp. 2301–2315, 2021.

[16] T. Hainsworth, L. Smith, S. Alexander, and R. MacCurdy, "A fabrication free, 3d printed, multi-material, self-sensing soft actuator," IEEE Robotics and Automation Letters, vol. 5, no. 3, pp. 4118–4125, 2020.

[17] G. B. Crowley, X. Zeng, and H.-J. Su, "A 3d printed soft robotic gripper with a variable stiffness enabled by a novel positive pressure layer jamming technology," IEEE Robotics and Automation Letters, vol. 7, no. 2, pp. 5477–5482, 2022.

[18] U. Yoo, Y. Liu, A. D. Deshpande, and F. Alamabeigi, "Analytical design of a pneumatic elastomer robot with deterministically adjusted stiffness," IEEE robotics and automation letters, vol. 6, no. 4, pp. 7773–7780, 2021.

[19] B. Parilusyan, M. Teyssier, Z. Guillaume, T. Charlet, C. Duhart, and M. Serrano, "Local layer splitting: An additive manufacturing method to define the mechanical properties of soft pneumatic actuators during fabrication," in 2023 IEEE International Conference on Robotics and Automation (ICRA). IEEE, 2023, pp. 12 331–12 337.

[20] D. Bauer, C. Bauer, A. Lakshmipathy, R. Shu, and N. S. Pollard, "Towards very low-cost iterative prototyping for fully printable dexterous soft robotic hands," in 2022 IEEE 5th International Conference on Soft Robotics (RoboSoft). IEEE, 2022, pp. 490–497.

[21] C. S. O'Bryan, T. Bhattacharjee, S. R. Niemi, S. Balachandar, N. Baldwin, S. T. Ellison, C. R. Taylor, W. G. Sawyer, and T. E. Angelini, "Three-dimensional printing with sacrificial materials for soft matter manufacturing," MRS bulletin, vol. 42, no. 8, pp. 571–577, 2017.

[22] S. Chen, W. S. Tan, M. A. Bin Juhari, Q. Shi, X. S. Cheng, W. L. Chan, and J. Song, "Freeform 3d printing of soft matters: recent advances in technology for biomedical engineering," Biomedical Engineering Letters, vol. 10, pp. 453–479, 2020.

[23] L. Friedrich and M. Begley, "Changes in filament microstructures during direct ink writing with a yield stress fluid support," ACS Applied Polymer Materials, vol. 2, no. 7, pp. 2528–2540, 2020.

[24] Lynxter, "3d printer manufacturer." [Online]. Available: https://lynxter.fr/en/

[25] D.-S. . shore A, "Dragon-skin 30 shore a silicone from smooth-on." [Online]. Available: https://www.smooth-on.com/products/dragon-skin-30/

[26] Simplify, "Advanced slicing software for 3d printing." [Online]. Available: https://www.simplify3d.com/

[27] J. Shintake, H. Sonar, E. Piskarev, J. Paik, and D. Floreano, "Soft pneumatic gelatin actuator for edible robotics," in 2017 IEEE/RSJ International Conference on Intelligent Robots and Systems (IROS). IEEE, 2017, pp. 6221–6226.

[28] F. Weigand, A. M. Nguyen, J. Wolff, and A. Seibel, "Toward industrial silicone 3d printing of soft robots," in 2021 IEEE 4th International Conference on Soft Robotics (RoboSoft). IEEE, 2021, pp. 523–526.